Spermatogenesis 2:2, 94-103; April/May/June 2012; © 2012 Landes Bioscience

Ontogenic development of spermatids during spermiogenesis in the high altitude bunchgrass lizard (*Sceloporus bicanthalis*)

Justin L. Rheubert,[1] Katherine Touzinsky,[2] Oswaldo Hernández-Gallegos,[3] Gisela Granados-González[3] and Kevin M. Gribbins[2,*]

[1]Department of Biology; St. Louis University; St. Louis, MO USA; [2]Deptartment of Biology; Wittenberg University; Springfield, OH USA; [3]Facultad de Ciencias; Universidad Autonoma del Estado de Mexico; Toluca, Mexico

Keywords: sperm, development, gametogenesis, lizard, microscopy

The body of ultrastructural data on spermatid characters during spermiogenesis continues to grow in reptiles, but is still relatively limited within the squamates. This study focuses on the ontogenic events of spermiogenesis within a viviparous and continually spermatogenic lizard, from high altitude in Mexico. Between the months of June and August, testicular tissues were collected from eight spermatogenically active bunchgrass lizards (*Sceloporus bicanthalis*) from Nevado de Toluca, México. The testicular tissues were processed for transmission electron microscopy and analyzed to access the ultrastructural differences between spermatid generations during spermiogenesis. Interestingly, few differences exist between *S. bicanthalis* spermiogenesis when compared with what has been described for other saurian squamates. Degrading and coiling membrane structures similar to myelin figures were visible within the developing acrosome that are likely remnants from Golgi body vesicles. During spermiogenesis, an electron lucent area between the subacrosomal space and the acrosomal medulla was observed, which has been observed in other squamates but not accurately described. Thus, we elect to term this region the acrosomal lucent ridge. This study furthers the existing knowledge of spermatid development in squamates, which could be useful in future work on the reproductive systems in high altitude viviparous lizard species.

Introduction

Spermatozoal morphology research over the last decade has provided a continual flow of ultrastructural data for reptiles. These studies have broadened the taxon sampling and some have even provided phylogenetic and evolutionary perspectives using gamete morphology.[1-4] Currently, the Iguania clade is the most highly sampled taxon in terms of ultrastructural characters,[5,6] with one study describing spermatozoal data for *Uta stansburiana* and *Urosaurus ornatus*[7] within the family Phrynosomatidae. These previous studies show that the Squamata contain multiple synapomorphies[8] but relationships between more recently derived taxonomic clades (i.e., genus, family level) are poorly elucidated and contain multiple points of convergence.[4,8] Vieira, Colli and Bao[1] showed that the Iguania contain relatively few apomorphic characters and the pleurodonta (Iguanidae, Crotaphytidae, Polychrotidae, Phrynosomatidae and Tropiduridae) only share one character, the presence of a perforatorial baseplate, which is also observed within Scleroglossa and the agamid, *Pogona barbata*. This character, however, may not have been presented or recognized in earlier published manuscripts leading to misinterpretation.

Unfortunately, the number of spermatid development studies does not parallel the unprecedented increase in mature sperm morphological data. Additional spermiogenic data within multiple species of lizards could lead to increases in morphological data sets as well as more insightful hypotheses concerning reproductive biology in squamates. Only a handful of studies exist that give complete ultrastructural descriptions of spermiogenesis within the Squamata.[9] These studies have shown both conserved characteristics (i.e., nuclear elongation, acrosome development via Golgi vesicles) as well as unique characters (i.e., rough endoplasmic reticulum involvement in acrosome formation;[10] the absence of manchette microtubules).[11] With each new study, important insights such as the number of Sertoli cells that are interacting with developing elongating spermatids,[12] become evident during germ cell development.

Within vertebrates, squamates have one of the most intricately structured acrosome complexes. The acrosome can be divided into an acrosomal cortex, acrosomal medulla, subacrosomal space, perforatorium, perforatorial base plate and nuclear rostrum. However, the developmental aspects are poorly understood due to the lack of taxon sampling and the constraints of microscopy on a seasonal event that occurs rapidly. Furthermore,

*Correspondence to: Kevin M. Gribbins; Email: kgribbins@wittenberg.edu
Submitted: 03/21/12; Revised: 04/16/12; Accepted: 04/16/12
http://dx.doi.org/10.4161/spmg.20410

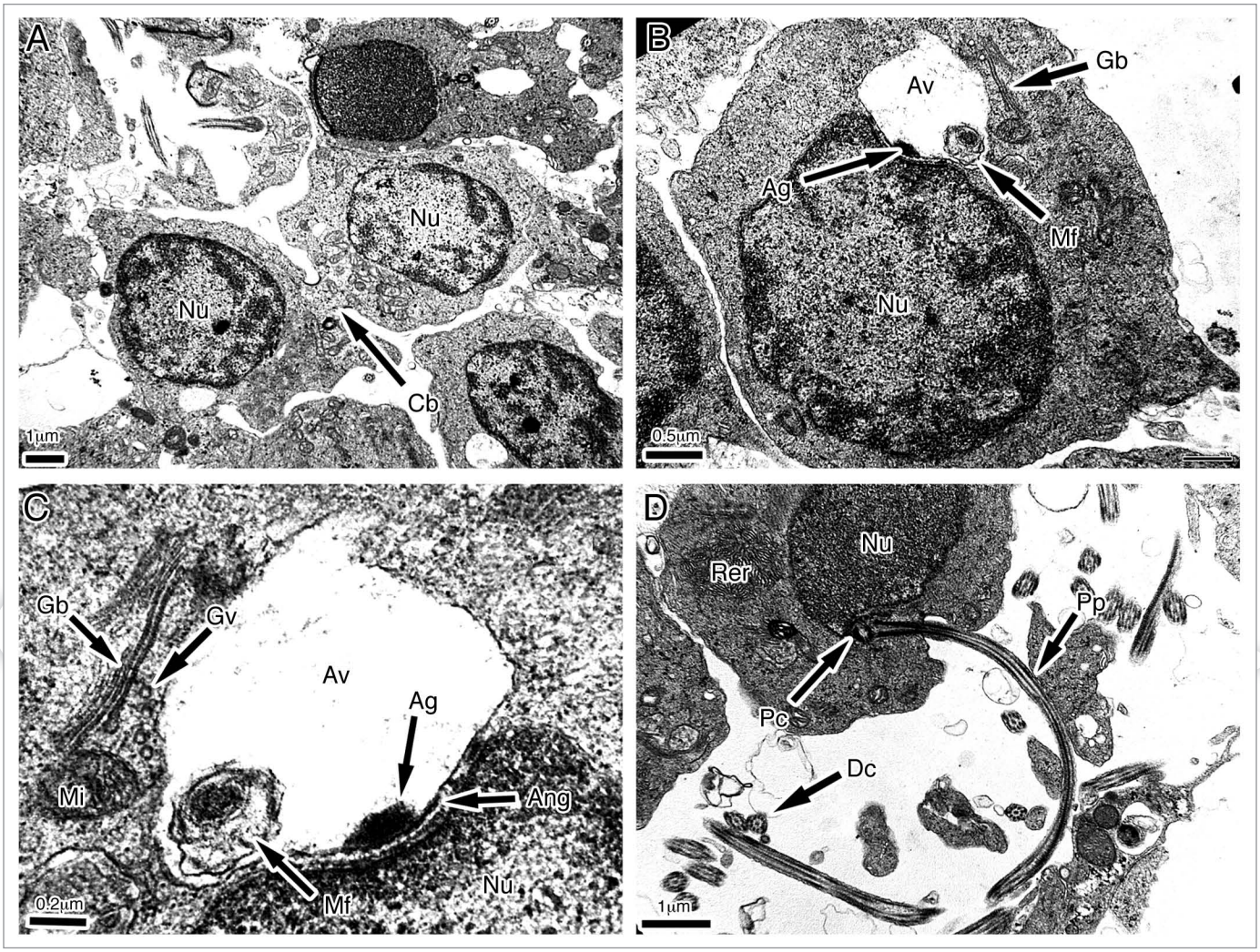

Figure 1. Round spermatids exhibiting the beginning stages of spermiogenesis. (A) Onset of spermiogenesis detailing cytoplasmic bridges (Cb) between germ cells. Nucleus (Nu). (B) As the acrosomal vesicle (Av) increases in size at the apex of the nucleus (Nu) a prominent Golgi body (Gb) can be seen juxtapositioned to the developing acrosome. (C) Multiple Golgi vesicles (Gv) budding from the cis portion of the Golgi body (Gb) merge with the acrosomal vesicle (Av) causing it to increase in size and multiple mitochondria (Mi) are seen in the lateral portions of the germ cell cytoplasm. Within the acrosomal vesicle (Av) the acrosomal granule (Ag) can be observed in its basal position and myelin figures (Mf) are situated within the acrosomal vesicle. (D) Early in development the proximal centriole (Pc) becomes situated at the basal portion of the nucleus (Nu) and the flagellum becomes elongated and the principal piece (Pp) can be distinguished. A cytoplasmic shift begins and rough endoplasmic reticulum (Rer) migrate away from the acrosomal complex.

the flagellum within Squamates and the Vertebrata is highly variable. Rheubert, McMahan, Sever, Bundy, Siegel and Gribbins[4] suggest flagellum morphology to be the most diverse region of spermatozoa within snakes. Yet again, the absence of taxon sampling yields limited amounts of data on potential developmental differences between species of squamates.

The purpose of this study is to investigate spermatid development within the seminiferous epithelium of *Sceloporus bicanthalis,* a spermatogenically aseasonal species (at elevations between 3,200 and 4,200 mm) from Central México.[13,14] Herein we present the first complete description of spermiogenesis in a phrynosomatid species and compare our findings with descriptions of spermiogenesis and mature spermatozoa in other squamate taxa, especially the Iguania.[15]

Results

The onset of spermiogenesis is manifested by the initial accumulation of round spermatids within the apical section of the seminiferous epithelium (**Fig. 1**). These spermatids are often in direct connection with each other via cytoplasmic bridges (**Fig. 1A-Cb**) where cytoplasm and organelle sharing occurs. The beginning stages of development are marked by the formation of an acrosomal vesicle (**Fig. 1B and C-Av**) adjacent to the nucleus (**Fig. 1B and C-Nu**). The Golgi apparatus (**Fig. 1B and C-Gb**) hosts budding vesicles (**Fig. 1C-Gv**) that originate from its proximal cisternum. These vesicles eventually merge at the apices of the nuclei (**Fig. 1B-Nu**) and are responsible for the acrosomal vesicles increase in size during early development. As

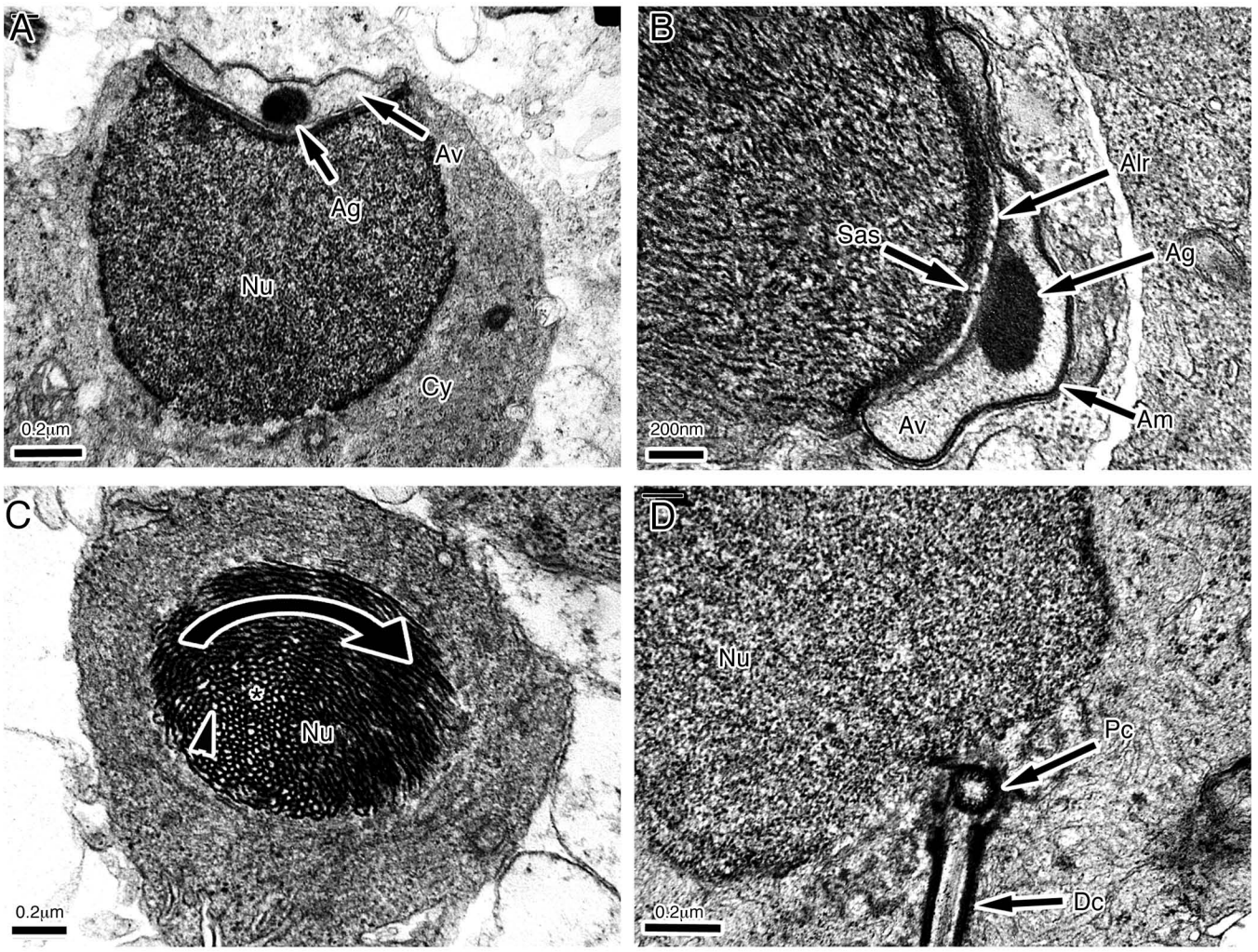

Figure 2. Early stages of chromatin condensation and elongation during spermiogenesis. (A) The germ cell migrates to the apical portion of the cytoplasm (Cy) pushing against the germ cell membrane causing the acrosome vesicle (Av) to flatten laterally. Acrosome granule (Ag), nucleus (Nu). (B) Between the acrosome vesicle (Av) and the membrane of the nucleus a dense protein layer forms and the subacrosomal space (Sas) becomes evident. The subacrosomal space is separated from the acrosomal complex by the acrosomal lucent ridge (Alr). Acrosomal granule (Ag). (C) During condensation of the nucleus (Nu) the chromatin condenses in both a granular (*) and spiral fashion (arrow) leaving open pits of nucleoplasm (arrowhead). (D) The proximal centriole (Pc) abuts against the condensing caudal nucleus (Nu) and the distal centriole (Dc) is is aligned perpendicular to the proximal centriole.

soon as the acrosomal vesicle makes full contact with the apex of the nucleus, a dark, rounded protein densification, the acrosomal granule, becomes visible (**Fig. 1B and C-Ag**). Within the acrosomal vesicle myelin figures are observed during the early stages of acrosomal development (**Fig. 1B and C-Mf**). During this stage of development an abundance of mitochondria (**Fig. 1C-Mi**) are observed apically along with rough endoplasmic recticulum (**Fig. 1D-ReR**), which are densely packed juxtapositioned to the nucleus (**Fig. 1D-Nu**). Flagellar development also starts early in spermiogenesis with the proximal (**Fig. 1D-Pc**) and distal centrioles of the developing flagellum becoming evident. The proximal centriole (**Fig. 1D-Pc**) is situated at the base of the nucleus and the distal centriole is abutted to the proximal centriole and elongated as the principal piece (**Fig. 1D-Pp**), which extends out into the lumen of seminiferous tubule.

As the round spermatid stage nears termination, the acrosomal granule and acrosomal vesicle have reached their maximum size. Several distinct patterns are visible in spermatid development that coincide with nuclear elongation (**Fig. 2**). The nucleus (**Fig. 2A-Nu**) migrates to the apical cytoplasm (**Fig. 2A-Cy**) causing the germ cell membrane and acrosomal membrane to be pushed together and appear as a single thickened membrane (**Fig. 2B-Am**). This forces the acrosome to flatten and elongate along the lateral sides of the nucleus (**Fig. 2B**). An initial dark-staining densification of protein termed the subacrosomal space (**Fig. 2B-Sas**) and an electron lucent space (**Fig. 2B-Alr**) become evident between the nuclear membrane and the inner acrosomal membrane. During this time the chromatin begins to condense in both a spiral (**Fig. 2C** and arrow) and granular (**Fig. 2C-***) fashion showing pits of open nucleoplasm (**Fig. 2C** and black arrowhead).

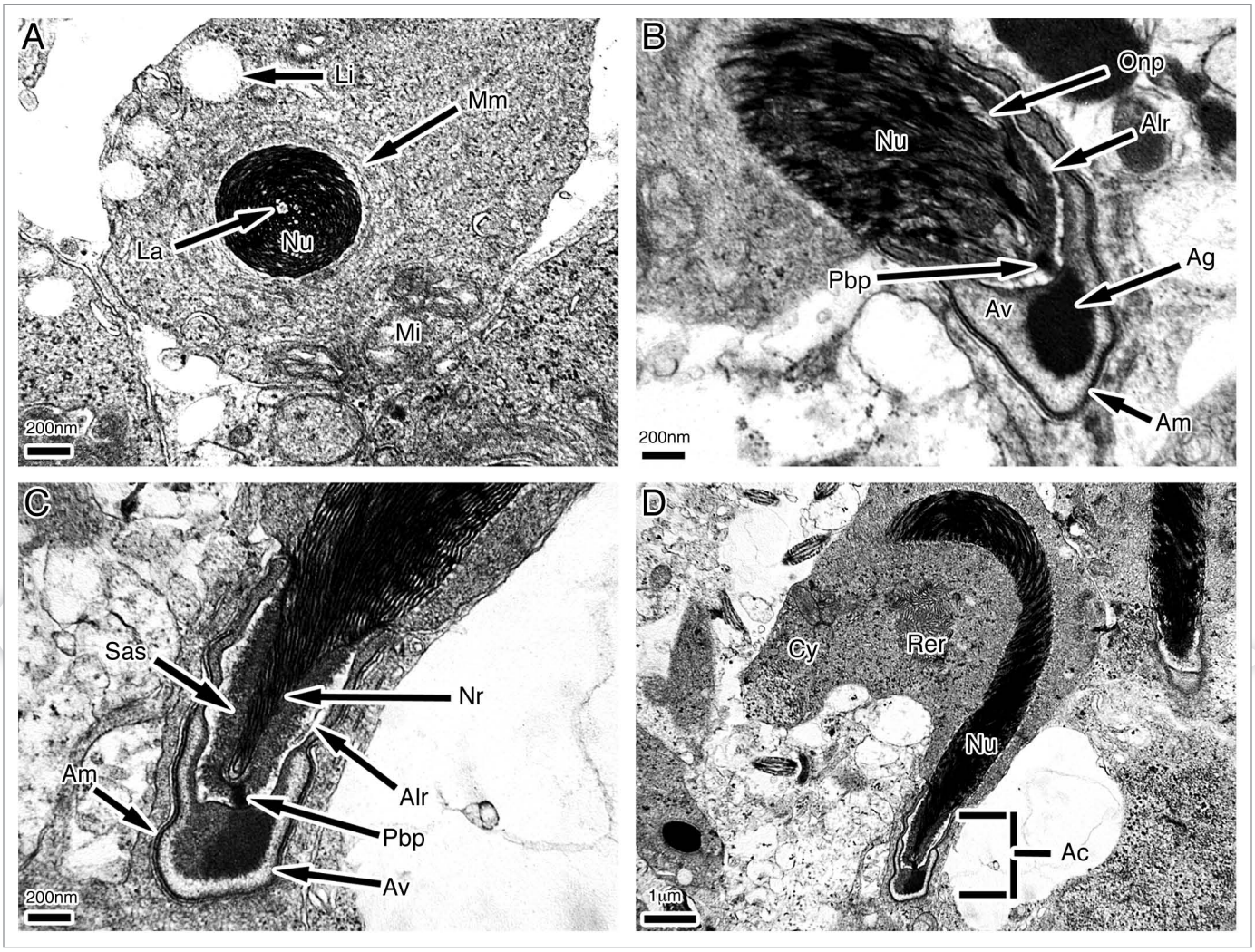

Figure 3. Chromosome condensation and elongation in step spermatids. (A) The chromatin of the nucleus (Nu) condenses around a central nuclear lacuna (La) while manchette microtubules (Mm) are arranged in an organized fashion around the nucleus. Multiple lipid inclusions (Li) and mitochondria (Mi) can be observed within the cytoplasm. (B) As the nucleus (Nu) condenses open pits of nucleoplasm (Onp) can be seen. During these stages the perforatorial base plate (Pbp) becomes dense just below the acrosomal lucent ridge (Alr). Acrosomal granule (Ag), acrosomal vesicle (Av), acrosomal membrane (Am). (C) As the acrosomal vesicle (Av) envelops the nucleus (Nu), the apical portion of the nucleus becomes laterally compressed and extends into the subacrosomal space (Sas) as the nuclear rostrum (Nr). Acrosomal lucent ridge (Alr), acrosomal Membrane (Am), perforatorial base plate (Pbp). (D) As the nucleus (Nu) elongates, it becomes arc shaped forcing the cytoplasm (Cy) and its contents such as rough endoplasmic reticulum (Rer) into the inner radius of the arc. Acrosomal complex (Ac).

The proximal centriole (**Fig. 2D-Pc**) rests at the base of the nucleus (**Fig. 2D-Nu**) and the distal centriole (**Fig. 2D-Dc**) aligns perpendicular to the proximal centriole at approximately 90 degrees.

Throughout chromatin condensation the nucleus (**Fig. 3A-Nu**) becomes more homogenous in electron density and the formation of the nuclear lacuna (**Fig. 3A-La**) is present with the chromatin spiraling around the lacuna during condensation. The bulk of elongation, aided by microtubules of the manchette (**Fig. 3A-Mm**), continues with a cytoplasmic shift posteriorly and, the acrosomal complex envelops the nucleus and becomes more differentiated (**Fig. 3B**). Located at the center of the subacrosomal space (**Fig. 3C-Sas**), is a dense and darkly staining perforatorial base plate (**Fig. 3B and C-Pbp**). Just apical to the subacrosomal space is a light layer of presumably open space that we elect to term the acrosomal lucent ridge (**Fig. 3B-Alr**). Throughout the process of nuclear elongation, the acrosome vesicle migrates laterally and squeezes along the sides of the nuclear rostrum (**Fig. 3C-Nr**), which extends into the subacrosomal space (**Fig. 3C-Sas**). The nucleus proper also continues elongating, which results in a thin, curved, spermatid nucleus. The curvature of the nucleus causes yet another cytoplasmic shift and the mitochondria (**Fig. 3D-Mi**) and rough endoplasmic recticulum (**Fig. 3D-Rer**) are forced to the inner radius of the nucleus (**Fig. 3D-Nu**).

During the late elongation stages of spermiogenesis the nucleus (**Fig. 4A-Nu**) becomes homogeneously condensed. The microtubules of the manchette (**Fig. 4A-Mm**) are visible in randomized congregations around the nucleus. As the spermatid matures, these microtubules align themselves into organized radials that

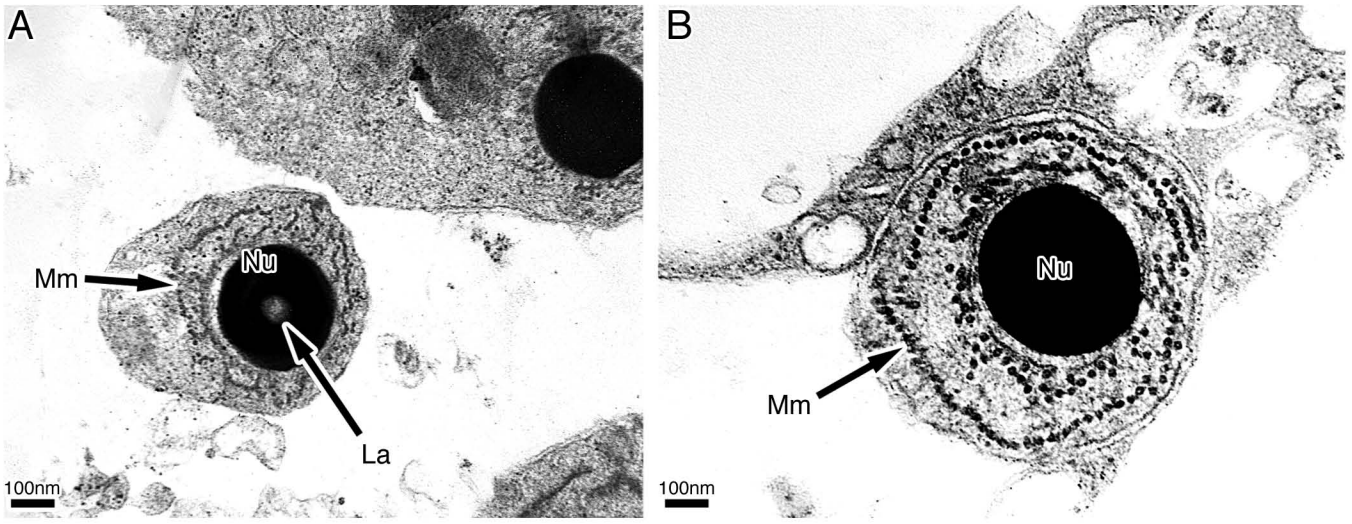

Figure 4. Manchette formation during late elongation of spermiogenesis. (A) The microtubules of the manchette (Mm) has an outer single ring of microtubules with disorganized groups of mirotubules found between this outer ring and the nuclear membrane (Nu). Nuclear lacuna (La). (B) Higher magnification of microtubule arrangement of the machette (Mm) around a cross section of the nucleus (Nu) of an elongating spermatid.

encircle the nucleus (**Fig. 4B**). The manchette microtubules in cross section are observed in a single outer circular layer with randomized congregations of microtubule groups between the outer microtubule ring and nuclear membrane.

Outside of the nucleus, the cytoplasm becomes reduced and is filled almost completely with mitochondria (**Fig. 5A-Mi**) and lipid inclusions (**Fig. 5A-Li**). The distal end of the nucleus (**Fig. 5B-Nu**) invaginates at the proximal centriole (Fig. 5B-Pc) forming the nuclear fossa (**Fig. 5B-Nf**), and the connection between the proximal and distal centrioles is sealed by the formation of the connecting piece (**Fig. 5B-Cp**). Mitochondria (**Fig. 5C-Mi**) migrate away from the nucleus toward the developing flagellum and are anchored intermittently by dense bodies (**Fig. 5C-Db**) that end with a terminal dense structure, the annulus (**Fig. 5C-An**). Densely stained fiber blocks making up the fibrous sheath (**Fig. 5C-Fs**) surround the axoneme beginning at mitochondrial tier two and extend past the annulus into the principal piece (**Fig. 5C and D-Pp**). Near the end of elongation, the germ cell cytoplasm containing copious amounts of mitochondria (**Fig. 5D-Mi**), rough endoplasmic reticulum (**Fig. 5D-Rer**) and lipid inclusions (**Fig. 5D-Li**) become completely isolated in the internal radial portion of the germ cell.

The result of spermiogenesis is a mature spermatid with mature structures (acrosome, elongated nucleus, flagellum). When the acrosome complex becomes fully differentiated, cross sectional views of the acrosome reveal lateral compression at its apical end (**Fig. 6C**) and a unilateral projection is observed at the most apical prospect. The acrosome is divided into the acrosomal medulla (**Fig. 6A and B-Acm**), acrosomal cortex (**Fig. 6A and B-Acc**), acrosomal lucent ridge (**Fig. 6A and C–E-Alr**), subacrosomal space (**Fig. 6A–D and F-Sas**), perforatorium (**Fig. 6A** inset, black arrowhead; **6B-Pe**), perforatorial base plate (not shown), and epinuclear lucent zone (**Fig. 6C-Elz**). Sertoli cells (**Fig. 6A, B and D-Sc**) can be seen enveloping the germ cell and show many ectoplasmic specializations (**Fig. 6E-Es**) between adjacent Sertoli cells. The chromatin is fully condensed and the nucleus is homogenous in density.

Distally, the flagellum is fully developed, positioned in the nuclear fossa (**Fig. 7B-Nf**), and displays the 9 + 3 microtubule arrangement (**Fig. 7B-9 + 3**). The midpiece (**Fig. 7C**) of the flagellum is surrounded by mitochondria (**Fig. 7C-Mi**) interspaced with dense bodies (**Fig. 7C-Db**). Peripheral fibers (**Fig. 7C-Pf**) are observed surrounding the axoneme and peripheral fibers 3 and 8 are grossly enlarged. A fibrous sheath (**Fig. 7C and D-Fs**) beginning at mitochondrial tier two surrounds the axoneme (**Fig. 7C and D**) and surrounds the entire principal piece (**Fig. 7D**). The fibrous sheath is discontinued distally within the flagellum to transition into the naked endpiece (**Fig. 7E**) where only the axoneme displaying the 9 + 2 microtubule arrangement is observed. However, the peripheral fibers associated with microtubule doublets 3 and 8 remain enlarged (**Fig. 7E-Pf**) even within the endpiece.

Discussion

Squamate spermiogenesis follows the same general steps (acrosome formation, nuclear condensation and elongation, and flagellar development) as all vertebrates (including reptiles: Iguania and Scleroglossa) studied to date[10,11,16,17] with *Sceloporus bicanthalis* being no exception. However, the addition of new taxa into the accumulating data of sperm morphology reveals new characters and new insights into the steps of sperm development. Many of the characters observed during developmental stages (i.e., acrosomal cortex, acrosomal medulla, acrosomal lucent ridge, perforatorium) are seen in the mature spermatozoa, which Rheubert, McMahan, Sever, Bundy, Siegel and Gribbins[4] showed to be extremely conserved, at least within ophidians.

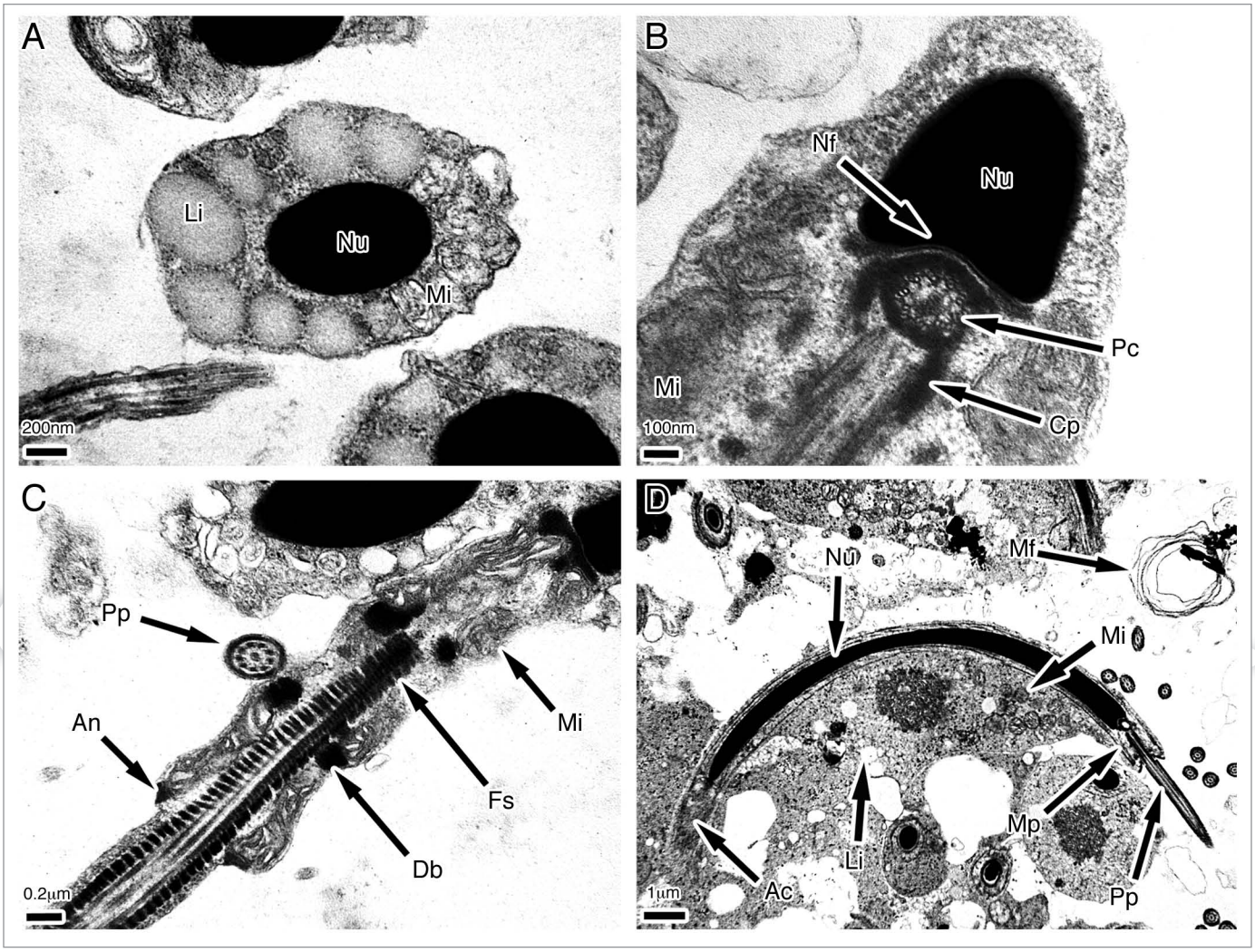

Figure 5. The final stages of elongation in late step spermatids. (A) As the nucleus (Nu) becomes homogenously electron dense multiple lipid inclusions (Li) and mitochondria (Mi) are observed within the cytoplasm. (B) The proximal centriole (Pc) is positioned within the nuclear fossa (Nf) and connected to the distal centriole via the connecting piece (Cp). (C) The flagellum becomes differentiated as mitochondria (Mi) and dense bodies (Db) surround the midpiece. A fibrous sheath (Fs) begins in the midpiece at mitochondrial tier two and continues into the principal piece (Pp). The transition between the principal piece and the endpiece in marked by a terminal dense structure, the annulus (An). (D) During the final stage of elongation the nucleus (Nu) is uniformly arc shaped and the lipid inclusions (Li), mitochondria (Mi) rough endoplasmic reticulum (Rer), and cytoplasm are forced to the inner radius of the arc. Midpiece (Mp), Principal piece (Pp).

During the early stages of sperm development, multiple cytoplasmic bridges can be seen between germ cells. These bridges aid in the communication of cells[18,19] by sharing gene products[20,21] which may cause them to develop together as a single cohort, a fundamental component to the germ cell development strategy observed in amphibians, squamates,[22,23] turtles,[24] and crocodilians.[25,26] During these early stages, the acrosome begins to develop from fusing Golgi vesicles similar to other amniotes studied to date.[27] Although Ferreira and Dolder[10] suggest the rough endoplasmic reticulum to be directly involved in acrosome development in *Iguana iguana*, the rough endoplasmic reticulum in *S. bicanthalis* is observed juxtapositioned to the nucleus and does not appear to be directly involved in acrosome formation. During acrosome formation multiple myelin figures are observed. The authors hypothesize these structures are degrading membrane delivered to the acrosome via the Golgi transport vesicles that are discarded during development. This process may occur by an ubiquitin modulated membrane protein that separates, joins, and/or cleaves excess membrane by the joining of two clathrin coated portions of acrosomal membrane. With the addition of membrane material (from fusing Golgi vesicles) the amount of membrane found surrounding the acrosome needs to decrease to further concentrate the hydrolytic enzymes and to allow the acrosome to remain tightly adhered to the nuclear body.

As the nucleus begins to condense the chromatin condenses in both a spiral and granular fashion similar to that found in the lizards *Iguana iguana*[10] and *Hemidactylus turcicus*[12] and the snake *Agkistrodon piscivorous*.[28] The lengthening of the nucleus is aided by microtubules of the machette which are present in every squamate species studied to date except *Anolis lineatopus*.[11] Typically

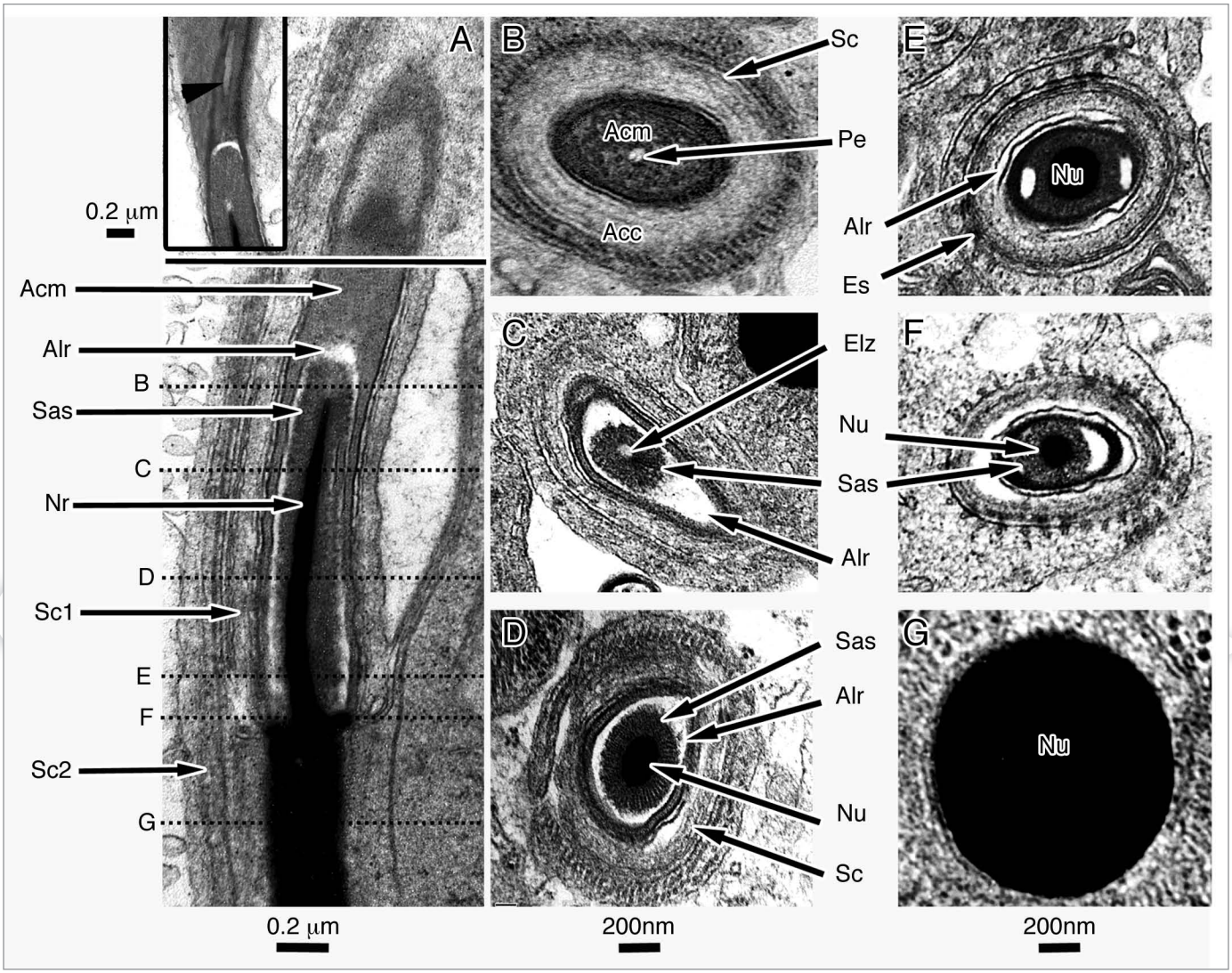

Figure 6. Apical portion of a mature spermatid prior to spermiation. (A) Sagittal view of the apical germ cell demonstrating the organization of the acrosomal complex into the acrosomal cortex (Acc), acrosomal medulla (Acm), acrosomal lucent ridge (Alr), subacrosomal space (Sas), nuclear rostrum (Nr) and surrounding Sertoli cells (Sc1 and Sc2). Inset: showing the perforatorium (Pe) in sagittal view. (B) Cross sectional view of the apex of the acrosom showing the perforatorium (Pe) extending into the acrosomal medulla (Acm). Acrosomal cortex (Acc), Sertoli cell (Sc). (C) Cross sectional view through the acrosome showing the epinuclear lucent zone (Elz) extending into the subacrosomal space (Sas). The acrosome is laterally compressed with a single ridge. Acrosomal lucent ridge (Alr). (D) Cross sectional view through the acrosome displaying the nuclear rostrum (Nu) extending into the subacrosomal space (Sas). Acrosomal lucent ridge (Alr), Sertoli cell (Sc). (E) Cross sectional view showing ectoplasmic specializations (Es) of the Sertoli cells. Acrosomal lucent ridge (Alr), nucleus (Nu). (F) Cross sectional view through the base of the acrosome displaying the nucleus (Nu) and subacrosomal space (Sas). (G) Cross sectional view through the nucleus (Nu).

in reptiles, the manchette is organized into a single or double inner circular layer and a well-developed, evenly distributed outer longitudinal layer of microtubules.[29] The manchette in *Sceloporus bicanthalis* is slightly different in that its longitudinal layer has an outer ring of microtubules and randomized groups of tubules between the outer ring and nuclear membrane. The functional or developmental significance of this unique arrangement is not known at this time. Also, during this late stage of development the nucleus arches forcing the contents of the cytoplasm to the inner radius of the nucleus. This may signify the beginning formation of the cytoplasmic residuum (Trauth S, personal communication).

The acrosome becomes further differentiated into multiple layers similar to other squamates.[1,12] A lucent structure separating the subacrosome space and the acrosomal cortex becomes evident. This structure is noted in all reptilian species studied to date (Rheubert JL, personal observation). However, this structure has been overlooked in many studies and inaccurately termed the acrosome vesicle,[30] subacrosomal clear zone[6] and the epinuclear lucent zone.[31] We elect to term this thin subacrosomal space the acrosomal lucent ridge to accurately describe its morphological features and distinguish the structure from the epinuclear lucent zone, which extends directly off the tip of the nuclear apex. This ridge is quite well developed in *S. bicanthalis* and is

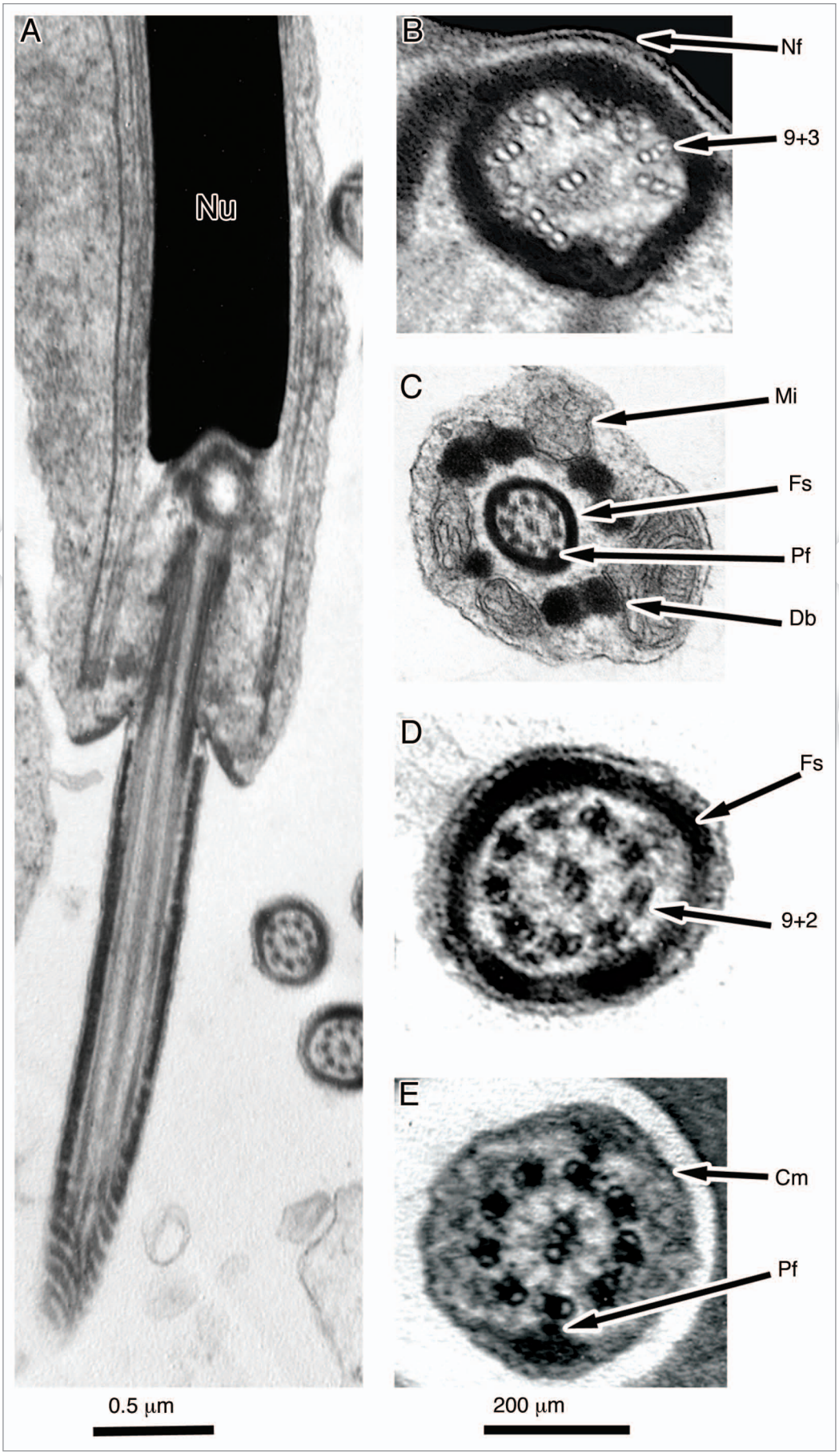

Figure 7. Posterior portion of a mature spermatid prior to spermiation. (A) Sagittal view of the spermatid nucleus (Nu). (B) Sagittal view of the proximal centriole displaying the 9 + 3 microtubule configuration situated in the nuclear fossa (Nf). (C) Cross sectional view of the midpiece showing the axoneme, in which peripheral fibers (Pf) 3 and 8 are grossly enlarged, and surrounded by the fibrous sheath (Fs). Mitochondria (Mi) separated by dense bodies (Db) surround the fibrous sheath. (D) Cross sectional view of the principal piece displaying the 9 + 2 microtubule arrangement and the fibrous sheath (Fs). (E) Cross sectional view of the endpiece displaying enlarged peripheral fibers (Pf) and the cell membrane (Cm).

very conspicuous in cross sections of the acrosomal complex (see **Fig. 6**).

During the late stages of development the nucleus becomes homogenously dense and most of the cytoplasm in packed within the inner radius of the nucleus. The cellular machinary begins to shift toward the flagellum as it becomes differentiated. The proximal centriole is adhered to the distal centriole via a connecting piece.[32] Mitochondria fill the midpiece separated by dense fibers and terminated at the annulus.

Prior to spermiation the spermatid resembles a mature spermatozoa (although this has yet to be investigated thoroughly). The acrosome is laterally compressed which resembles that of other taxa within Iguania.[1,5,33,34] A single perforatorium, a suggested synapomorphy for the squamata[4,34] extends into the acrosomal medulla. Separating the acrosomal medulla and the subacrosomal space, which has previously been termed the subacrosomal cone in multiple studies, is a lucent region which we term the acrosomal lucent ridge. An epinuclear lucent region is present similar to all squamates with the exception of the Scincomorpha[5,12,31] and the Gekkonid *Heternotia binoei*.[31] A nuclear lacuna is present which appears to be variable among taxa (Rheubert JL, personal observation). However, the nuclear lacuna does not penetrate the entire nucleus and thus may have been missed in previous studies. The midpiece region is relatively short with the fibrous sheath beginning at mitochondria tier two which is consistent among phrynosomatids[7] but differs among other Iguania taxa.[5,33,35]

Throughout spermiogenesis and prior to spermiation the germ cells can be seen enveloped by multiple Sertoli cells. Previous literature suggests these cells are involved in providing nourishment for the germ cell.[36] In mammals, the Sertoli cell ultrastructure differs depending on the stage of germ cell development the sustenacular cell is associated with[37] (e.g., Sertoli cells associated with spermatids differ than those associated with spermatogonia). However, with the germ cell development strategy employed by reptiles,[9] a single Sertoli cell can be associated with multiple germ cell development stages.[12] The Sertoli cells are anchored to the germ cells via ectoplasmic specializations and multiple zonula adherens are observed between juxtapositioned Sertoli cells.[38] Although Rheubert, Siegel, Venable, Sever and Gribbins[12] demonstrated that Sertoli cells displayed different cytoplasmic properties, which was also evident in *Sceloporus bicanthalis*, the function of this is not understood and warrants further investigation.

Overall, spermiogenesis in *Sceloporus bicanthalis* resembles that of other amniotes. Although no single autapomorphies were observed for this species, new structural data concerning sperm development in a squamate species was added. Rheubert, McMahan, Sever, Bundy, Siegel and Gribbins,[4] in their study on ophidians, stated that a unique combination of various characters may be the differentiation between species. However, more data are needed in order to test this hypothesis across all squamate species. Furthermore, since previous authors have stated spermatozoon morphology is species specific these data may help to clarify taxonomic discrepencies especially between *Sceloporus bicanthalis* and *Sceloporus aeneus*,[39] which are considered sister taxa.

Materials and Methods

Animal collection. Eight sexually mature male *Sceloporus bicanthalis* were selected based on spermiogenic activity[14] and were collected between the months of June and August from a study area near the top of the Nevado de Toluca volcano in Mexico (19° 07' 30''N, 99° 46' 15''W; 4,200 mm above sea level). Specimens were sacrificed and testes were immediately removed, minced into small fragments and submerged in Trump's Fixative (EMS). Once submerged, they were transferred to fresh fixative and kept under refrigeration (4°C) for at least 48 h.

Tissue preparation. Tissue fragments were homogenized into 2–3 mm blocks and washed twice with cacodylate buffer solution (pH 7.0) for 20 min each. Washed tissues were post-fixed in 2% osmium tetroxide for 2 h, washed with three rounds of cacodylate buffer (pH 7.0, 20 min each), dehydrated in a series of graded ethanol (70%, 85%, 90%, 95% and 100% X2), and cleared with two ten-minute treatments of propylene oxide. After initial prep, tissues were slowly introduced to epoxy resin (Embed 812, EMS) (2:1 and 1:1 solutions of propylene oxide: epoxy resin). Finally, the samples were placed in pure Embed 812 for 24 h and embedded in fresh resin in small beam capsules. The capsules were cured for 48 h at 70°C in a Fisher isotemperature vacuum oven (Fisher Scientific). Once hardened, 90 nm sections were obtained via a diamond knife (DDK) and an LKB automated ultramicrotome (LKB Produkter AB). Sections were placed on copper grids and stained for 15 min with uranyl acetate and 5 min with lead citrate.

Ultrastructural analysis. Samples were viewed under a JEOL JEM-1200EX II transmission electron microscope (JEOL Inc.). Representative spermatids within the seminiferous epithelium and relevant structural components associated with spermiogenesis were located and photographed using a Gatan 785 Erlangshen digital camera (Gatan). The micrographs were analyzed and composite plates were assembled using Adobe Photoshop CS (Adobe Systems).

Disclosure of Potential Conflicts of Interest

No potential conflicts of interest were disclosed.

Acknowledgements

The authors would like to thank Anthony J. Wilmes for proofreading an earlier draft of this manuscript. Funding was provided by competitive research grants through Wittenberg University. Financial support for lizard collections and research was provided to Gisela Granados-González and Oswaldo Hernández-Gallegos through PIFI.

References

1. Vieira GH, Colli GR, Báo SN. The ultrastructure of the spermatozoon of the lizard *Iguana iguana* (Reptilia, Squamata and Iguanidae) and the variability of sperm morphology among iguanian lizards. J Anat 2004; 204:451-64; PMID:15198687; http://dx.doi.org/10.1111/j.0021-8782.2004.00300.x.
2. Tourmente M, Cardozo G, Bertona M, Guidobaldi A, Giojalas L, Chiaraviglio M. The ultrastructure of the spermatozoa of *Boa constrictor occidentalis*, with considerations on its mating system and sperm competition theories. Acta Zoologica 2006; 87:25-32; http://dx.doi.org/10.1111/j.1463-6395.2006.00217.x.
3. Tavares-Bastos L, Colli G, Báo S. The evolution of sperm ultrastructure among Boidae (Serpentes). Zoomorphology 2008; 127:189-202; http://dx.doi.org/10.1007/s00435-008-0062-8.
4. Rheubert JL, McMahan CD, Sever DM, Bundy MR, Siegel DS, Gribbins KM. Ultrastructure of the reproductive system of the black swamp snake (*Seminatrix pygaea*). VII. spermatozoon morphology and evolutionary trends of sperm characters in snakes. J Zoo Syst Evol Res 2010; 48:366-75; http://dx.doi.org/10.1111/j.1439-0469.2010.00573.x.
5. Teixeira RD, Colli GR, Báo SN. The ultrastructure of spermatozoa of the lizard *Polychrus acutirostris* (Squamata and Polychrotidae). J Submicrosc Cytol Pathol 1999; 31:387-95.
6. Ferreira A, Dolder H. Sperm ultrastructure and spermatogenesis in the lizard, *Tropidurus itambere*. Biocell 2003; 27:353-62; PMID:15002752.
7. Scheltinga DM, Jamieson BMG, Trauth SE, McAllister CT. Morphology of the spermatozoa of the iguanian lizards *Uta stansburiana* and *Urosaurus ornatus* (Squamata and Phrynosomatidae). J Submicrosc Cytol 2000; 31:387-95.
8. Jamieson BMG. The ultrastructure of spermatozoa of the Squamata (Reptilia) with phylogenetic considerations. In: Jamieson BMG, Ausio J, Justine JL, Eds. Advances in Spermatozoal Phylogeny and Taxonomy. Paris: Mémoires du Muséum national d'Histoire Naturelle 1995; 359-83.
9. Gribbins KM. Reptilian spermatogenesis: A histological and ultrastructural perspective. Spermatogenesis 2011; 1:250-69; PMID:22319673; http://dx.doi.org/10.4161/spmg.1.3.18092.
10. Ferreira A, Dolder H. Ultrastructural analysis of spermiogenesis in *Iguana iguana* (Reptilia: Sauria: Iguanidae). Eur J Morphol 2002; 40:89-99; PMID:12854047; http://dx.doi.org/10.1076/ejom.40.2.89.15452.
11. Rheubert JL, Wilson BS, Wolf KW, Gribbins KM. Ultrastructural study of spermiogenesis in the Jamaican Gray Anole, *Anolis lineatopus* (Reptilia: Polychrotidae). Acta Zoologica 2010; 91:484-94; http://dx.doi.org/10.1111/j.1463-6395.2009.00446.x.
12. Rheubert JL, Siegel DS, Venable KJ, Sever DM, Gribbins KM. Ultrastructural description of spermiogenesis within the Mediterranean Gecko, *Hemidactylus turcicus* (Squamata: Gekkonidae). Micron 2011; 42:680-90; PMID:21543229; http://dx.doi.org/10.1016/j.micron.2011.03.006.
13. Hernández-Gallegos O, Méndez-de la Cruz FR, Villagrán-Santa Cruz M, Andrews RM. Continuous spermatogenesis in the lizard *Sceloporus bicanthalis* (Sauria: Phrynosomatidae) from high elevation habitat of central Mexico. Herpetologica 2002; 58:415-21; http://dx.doi.org/10.1655/0018-0831(2002)058[0415:CSITLS]2.0.CO;2.
14. Gribbins K, Anzalone M, Collier M, Granados-González G, Villagrán-Santa Cruz M, Hernández-Gallegos O. Temporal germ cell development strategy during continuous spermatogenesis within the montane lizard, *Sceloporus bicanthalis* (Squamata; Phrynosomatidae).Theriogenology 2011; 76:1090-9; PMID:21752450; http://dx.doi.org/10.1016/j.theriogenology.2011.05.015.
15. Conrad JL. Phylogeny and systematics of squamata (reptilia) based on morphology. B Am Mus Nat Hist 2008; 1-182.
16. Russell LD, Hikim SAP, Ettlin RA, Legg ED. Histological and Histopathological Evaluation of the Testis. Clearwater, FL: Cache River Press 1990.
17. Healy JM, Jamieson BGM. The ultrastructure of spermatogenesis and epididymal spermatozoa of the Tuatara *Sphenodon punctatus* (Sphenodontida and Amniota). Philos Trans R Soc Lond B Biol Sci 1994; 344:187-99; http://dx.doi.org/10.1098/rstb.1994.0060.
18. Fawcett DW, Ito S, Slautterback D. The occurrence of intercellular bridges in groups of cells exhibiting synchronous differentiation. J Biophys Biochem Cytol 1959; 5:453-60; PMID:13664686; http://dx.doi.org/10.1083/jcb.5.3.453.
19. Dym M, Fawcett DW. Further observations on the numbers of spermatogonia, spermatocytes and spermatids connected by intercellular bridges in the mammalian testis. Biol Reprod 1971; 4:195-215; PMID:4107186.
20. Braun RE, Behringer RR, Peschon JJ, Brinster RL, Palmiter RD. Genetically haploid spermatids are phenotypically diploid. Nature 1989; 337:373-6; PMID:2911388; http://dx.doi.org/10.1038/337373a0.
21. Morales CR, Wu XQ, Hecht NB. The DNA/RNA-binding protein, TB-RBP, moves from the nucleus to the cytoplasm and through intercellular bridges in male germ cells. Dev Biol 1998; 201:113-23; PMID:9733578; http://dx.doi.org/10.1006/dbio.1998.8967.
22. Gribbins KM, Rheubert JL, Collier MH, Siegel DS, Sever DM. Histological analysis of spermatogenesis and the germ cell development strategy within the testis of the male western Cottonmouth Snake, *Agkistrodon piscivorus leucostoma*. Annals of Anatomy. Anat Anz 2008; 190:461-76; http://dx.doi.org/10.1016/j.aanat.2008.07.003.
23. Rheubert JL, McHugh HH, Collier MH, Sever DM, Gribbins KM. Temporal germ cell development strategy during spermatogenesis within the testis of the Ground Skink, *Scincella lateralis* (Sauria: Scincidae). Theriogenology 2009; 72:54-61; PMID:19344944; http://dx.doi.org/10.1016/j.theriogenology.2009.01.021.
24. Gribbins KM, Gist DH, Congdon JD. Cytological evaluation of spermatogenesis and organization of the germinal epithelium in the male slider turtle, *Trachemys scripta*. J Morphol 2003; 255:337-46; PMID:12520551; http://dx.doi.org/10.1002/jmor.10069.
25. Gribbins KM, Elsey RM, Gist DH. Cytological evaluation of the germ cell development strategy within the testis of the American alligator, *Alligator mississippiensis*. Acta Zoologica 2006; 87:59-69; http://dx.doi.org/10.1111/j.1463-6395.2006.00220.x.
26. Wang L, Wu X, Xu D, Wang R, Wang C. Development of testis and spermatogenesis in *Alligator sinensis*. J Appl Anim Res 2008; 34:23-8; http://dx.doi.org/10.1080/09712119.2008.9706934.
27. Gribbins KM, Rheubert JL. The ophidian testis, spermatogenesis and mature spermatozoa. In: Aldridge RD, Sever DM, Eds. Reproductive Biology and Phylogeny of Snakes. Boca Raton, Fl: CRC Press 2011; 183-264.
28. Gribbins KM, Rheubert JL, Anzalone ML, Siegel DS, Sever DM. Ultrastructure of spermiogenesis in the Cottonmouth, *Agkistrodon piscivorus* (Squamata: Viperidae: Crotalinae). J Morphol 2010; 271:293-304; PMID:19827154.
29. Gribbins KM, Mills EM, Sever DM. Ultrastructural examination of spermiogenesis within the testis of the ground skink, *Scincella laterale* (Squamata, Sauria and Scincidae). J Morphol 2007; 268:181-92; PMID:17154286; http://dx.doi.org/10.1002/jmor.10505.
30. Colli GR, Teixeira RD, Scheltinga DM, Mesquita DO, Wiederhecker HC, Báo SN. Comparative study of sperm ultrastructure of five species of teiid lizards (Teiidae and Squamata) and *Cercosaura ocellata* (Gymnophthalmidae and Squamata). Tissue Cell 2007; 39:59-78; PMID:17331552; http://dx.doi.org/10.1016/j.tice.2006.12.001.
31. Jamieson BGM, Oliver SC, Scheltinga DM. The Ultrastructure of the Spermatozoa of Squamata—I. Scincidae, Gekkonidae and Pygopodidae (Reptilia). Acta Zoologica 1996; 77:85-100; http://dx.doi.org/10.1111/j.1463-6395.1996.tb01255.x.
32. Bloom W, Fawcett DW. A Textbook of Histology. Philadelphia, PA: W.B. Saunders Company 1975.
33. Vieira GHC, Colli GR, Báo SN. Phylogenetic relationships of corytophanid lizards (Iguania, Squamata and Reptilia) based on partitioned and total evidence analyses of sperm morphology, gross morphology and DNA data. Zool Scr 2005; 34:605-25; http://dx.doi.org/10.1111/j.1463-6409.2005.00208.x.
34. Jamieson BG, Koehler L, Todd BJ. Spermatozoal ultrastructure in three species of parrots (aves and Psittaciformes) and its phylogenetic implications. Anat Rec 1995; 241:461-8; PMID:7604961; http://dx.doi.org/10.1002/ar.1092410404.
35. Vieira GHC, Cunha LD, Scheltinga DM, Glaw F, Colli GR, Báo SN. Sperm ultrastructure of hoplocercid and oplurid lizards (Sauropsida, Squamata and Iguania) and the phylogeny of Iguania. J Zoo Syst Evol Res 2007; 45:230-41; http://dx.doi.org/10.1111/j.1439-0469.2007.00406.x.
36. Wang RS, Yeh S, Chen LM, Lin HY, Zhang C, Ni J, et al. Androgen receptor in sertoli cell is essential for germ cell nursery and junctional complex formation in mouse testes. Endocrinology 2006; 147:5624-33; PMID:16973730; http://dx.doi.org/10.1210/en.2006-0138.
37. Skinner MK. Sertoli cell-somatic cell interactions. In: Skinner MK, Griswold MD, Eds. Sertoli Cell Biology. London: Elsevier Academic Press 2005; 317-28.
38. Grove BD, Vogl AW. Sertoli cell ectoplasmic specializations: a type of actin-associated adhesion junction? J Cell Sci 1989; 93:309-23; PMID:2515196.
39. Benabib M, Kjer KM, Sites JW. Mitochondrial DNA sequence-based phylogeny and the evolution of viviparity in the *Sceloporus scalaris* group (Reptilia and Squamata). Evolution 1997; 51:1262-75; http://dx.doi.org/10.2307/2411055.